Dextran-covered pH-sensitive oily core nanocapsules produced by interfacial Reversible Addition-Fragmentation chain transfer miniemulsion polymerization

Laura Marcela Forero Ramirez, Ariane Boudier, Caroline Gaucher, Jerome Babin, Alain Durand, Jean-Luc Six, Cécile Nouvel

Dextran-covered pH-sensitive oily core nanocapsules produced by interfacial Reversible Addition-Fragmentation Chain Transfer miniemulsion polymerization

Laura Marcela FORERO RAMIREZ[a], Ariane BOUDIER[b], Caroline GAUCHER[b], Jérôme BABIN[a], Alain DURAND[a], Jean-Luc SIX[a], Cécile NOUVEL[a]*±

[a]Université de Lorraine, CNRS, LCPM, F-54000 Nancy, France

[b]Université de Lorraine, CITHEFOR EA 3452, Nancy F-54001, France

± Current address Université de Lorraine, CNRS, LRGP, F-54000 Nancy, France

Correspondence to: Cécile Nouvel (E-mail: cecile.nouvel@univ-lorraine.fr)

Fax : 33(0) 3 83 32 29 75; Tel : 33(0) 3 72 74 38 32

Additional Supporting Information will be found in the online version of this article.

ABSTRACT

Aiming to prepare oily core pH-sensitive nanocapsules (NCs) for anticancer drugs delivery, the use of a dextran-based transurf ($DexN_3$-$\tau CTA\gamma$) as both stabilizer and macromolecular chain transfer agent in methyl methacrylate/2-(diethylamino)ethyl methacrylate (MMA/DEAEMA) miniemulsion copolymerization was investigated. NCs of about 195 nm with an oily-core of Miglyol 810 (M810) and a dextran coverage covalently linked to the poly(MMA-co-DEAEMA) intern shell have been obtained. Compared to the non-sensitive PMMA-based NCs (prepared in a similar way), these novel objects were shown to swell in acidic media and to trigger Coumarin 1 release in physiological relevant pH range. As a starting point of NCs biological effects, cytotoxicity and NCs-proteins interactions studies were performed with both PMMA and poly(MMA-co-DEAEMA)-based NCs. Finally, free azide functions from dextran-based coverage were successfully exploited to attach fluorescent model dyes to NCs surface. The overall results suggest that this novel NCs platform could be potentially used as drug nanocarriers for intravenous injection.

1. INTRODUCTION

The design of nanoparticle-based platforms for anti-cancer drug delivery has proven to be challenging as several physiological constraints need to be addressed [1], [2]. In particular, for parenteral administration, drug delivery systems (DDS) are expected to: i) be stable in circulation, ii) have neutral and hydrophilic surface to minimize interaction with blood components iii) not accumulate in non-pathological tissue, iv) not be cleared too fastly by the kidneys, v) have reduced toxicity and vi) provide controlled, sustained and specific drug release. In addition, for most DDS platforms, the circulation time should be maximized to increase accumulation in the tumor through the Enhanced Permeability and Retention effect, commonly called passive targeting [3], [4]. Moreover, possible incorporation of ligands at DDS surface enables a specific targeting of pathological cells, usually called active targeting. In this respect, DDS having polysaccharide coverage are particularly interesting. In fact, polysaccharides possess many functions along their backbones, as hydroxyls for instance, which can easily be functionalized by grafting ligands [5]. Furthermore, some polysaccharides such as dextran are nontoxic, hydrophilic, biocompatible and biodegradable, which make them suitable for biomedical applications [6].

Our team recently developed a suitable one-step technique to produce oily core nanocapsules (NCs) having irreversibly anchored dextran coverage. The approach consisted in the use of a multifunctional dextran-based reactive surfactant acting as stabilizer as well as initiator (Inisurf) [7] or chain transfer agent (Transurf) [8] to perform Atom Transfer Radical Polymerization or Reversible Addition-Fragmentation chain Transfer (RAFT) polymerization in miniemulsion, respectively. Figure 1 shows the preparation of dextran-covered oily core NCs by RAFT miniemulsion polymerization using a dextran-based transurf. Because of its amphiphilic character, such transurf was able to migrate at the oil/water interface to mediate there the polymerization from their reactive groups, so producing grafted copolymers. Grafts constituting NCs internal shell were found to have well-defined macromolecular parameters as reported in our recent manuscript [8].

In recent years, the design of smart DDS has attracted increasing attention because of their ability to control drug release in response to specific internal (temperature, pH, enzymes or redox gradients) or external stimuli (temperature, magnetic field, ultrasound intensity, light or electric pulses) [9], [10]. Poly[2-(diethylamino)ethyl methacrylate] (PDEAEMA) is a biocompatible

weak polybase with a pKa of about 7.3 [11] already tested in pH-responsive systems. Thus we hypothesized that the incorporation of 2-(diethylamino)ethyl methacrylate (DEAEMA) in NCs formulation would confer pH-responsiveness to the NC polymeric shell in physiological pH range (4.5-7.4). Accordingly, this would allow a pH-triggered release of drug in the acidic tumor microenvironment or intracellular compartments [12]. In this regard, our previous studies on RAFT miniemulsion polymerization of methyl methacrylate (MMA) using a dextran-based transurf would be extended here to the miniemulsion copolymerization of MMA with DEAEMA to produce dextran-covered oily-core NCs having a poly(MMA-co-DEAEMA) shell. To the best of our knowledge, most of the studies devoted to the RAFT (co)polymerization of DEAEMA were carried out in homogeneous media using molecular RAFT agents [13]–[25]. There is only one work dealing with the styrene emulsion polymerization using a preformed DEAEMA-based macromolecular Chain Transfer Agent (macroCTA) [26]. Some studies reported the use of DEAEMA as (co)monomer in a free radical emulsion polymerization process [27]–[32], to mostly produce pH-sensitive nanogels. Herein and in an original way, we reported a new synthesis protocol to create dextran-coated biocompatible NCs (with a hydrophobic oil core) that are both pH-sensitive and surface functionalizable, thus being potentially very interesting as drug carriers, e.g. for cancer therapy. To the best of our knowledge, those are the first pH-sensitive oily core NCs and even more dextran-covered smart NCs.

The present work was firstly focused on poly(MMA-co-DEAEMA)-based oily core NCs formulation by RAFT polymerization in heterogeneous conditions (miniemulsion polymerization) using a dextran-based transurf. These NCs were evaluated as DDS for parenteral administration. Both PMMA- and poly(MMA-co-DEAEMA)-based NCs (named PMMA-NCs and COPO-NCs, respectively) have been examined in terms of surface-charge, dextran coverage, colloidal stability, and physicochemical behavior under pH variations. The potential of such NCs to encapsulate and release hydrophobic substances was evidenced with a model fluorescent dye. In addition, investigation of NCs interactions with blood proteins and of cytotoxicity towards human monocytes was performed *in vitro*. Finally, fluorescent labeling of NCs was experienced to confirm the possible NCs surface modification for the selective targeting of cancer cells.

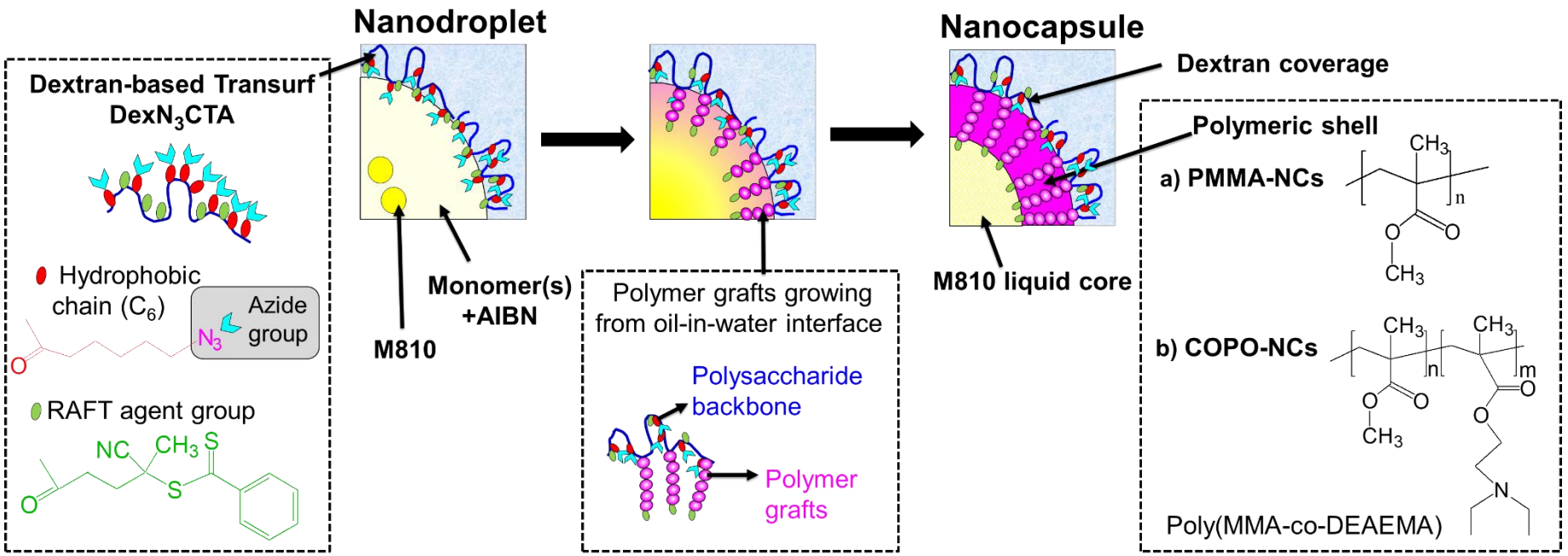

Figure 1. Preparation of dextran-covered oily core NCs by RAFT miniemulsion (co)polymerization using a dextran-based transurf ($DexN_3CTA$).

2. EXPERIMENTAL SECTION

2.1 Materials and methods

Dextran T40 ($\bar{M}_n$ = 26 000 g/mol, Đ = 1.3; values determined by size exclusion chromatography coupled to a multi-angle laser light scattering (SEC-MALLS) in DMSO/$NaNO_3$ (0,1 M)) was purchased from Aldrich. Produced from Leuconostoc mesenteroides B 512-F, it was having very low branching (< 5% as given by the furnisher) and could be considered as linear. Methyl methacrylate (MMA, 99% Aldrich) and 2-(diethylamino)ethyl methacrylate (DEAEMA, 99% Aldrich) were vacuum distilled from CaH_2. 2,2-azobis(isobutyronitrile) (AIBN, 99%, Aldrich) was purified by recrystallization from methanol. Miglyol®810 (M810, d = 0.94 g/cm^3, viscosity = 28 mPa.s, water content: 0.02 wt%) was a gift from CREMER Oleo GmbH & Co. division. 4-Carbethoxy-7-propargyloxy-coumarin (Cou-click) was prepared using literature with slight modifications [33]. 7-Diethylamino-4-methylcoumarin (Cou1, 99%-Aldrich), dibenzocyclooctyne-PEG_4-Fluor545 (DBCO-PEG_4-TAMRA, 90%-Aldrich), Sodium Dodecyl Sulfate (SDS, 99%-Aldrich) and ethylenediaminetetraacetic acid (EDTA, 99%-Aldrich) were used without further purification. Bovine Serum Albumin (BSA), fibrinogen from human plasma, RPMI 1640, fetal bovine serum, penicillin, streptomycin and amphotericin B, were all of analytic grade and purchased from Aldrich. Cell proliferation reagent 4-[3-(4-Iodophenyl)-2-(4-nitrophenyl)-2H-5-tetrazolio]-1,3-benzene disulfonate (WST-1) was supplied by Roche.

Phosphate-buffered saline solution (PBS) was prepared as follows: [Na_2HPO_4] = 6.48 × 10^{-3} M, [KH_2PO_4] = 1.47 × 10^{-3} M, [NaCl] = 138 × 10^{-3} M, and [KCl] = 2.68 × 10^{-3} M, final pH adjusted to 7.4. Ultrapure deionized water (>18.2 MΩ.cm) was used for the preparation of all solutions.

Dextran-based transurfs called $DexN_3$-τCTAγ were synthesized in two steps as previously described [8]. τ and γ were the number of N_3-end alkyl chains and of dithiobenzoate chain transfer agent groups (CTA) introduced per 100 glucopyranosic units, respectively.

2.2 RAFT miniemulsion (co)polymerization

Experimental conditions were inspired from our previous work [8]. $[DexN_{3\text{-}20}CTA_{3.7}]_0$=10 g/L and $[\text{CTA groups}]_0/[\text{AIBN}]_0$ molar ratio was fixed to 3. 150 mg of $DexN_{3\text{-}20}CTA_{3.7}$ were dissolved in 15 mL of MilliQ water. For MMA homopolymerization, the organic phase was composed of 1.1 mL (10.3 mmol) of MMA, 275 µL of M810 and 1.3 mg (7.9×10^{-3} mmol) of AIBN. In the case of

MMA/DEAEMA copolymerization, 0.3 mL of MMA (2.9 mmol) and 1.7 mL of DEAEMA were used, all other quantities being the same. DEAEMA was added in excess because of its higher water solubility (67 g/mL as estimated by us). So, from 1.7 mL of DEAEMA, 1.1 mL and 0.6 mL (3.8 mmol) split into the aqueous and organic phases, respectively. For encapsulation experiments, 21 mg of Cou1 (0.09 mmol) were added to the organic phase.

The aqueous phase was poured into the organic phase and the mixture was sonicated in an ice bath during 2 min (51% amplitude (power 46W), pulsed mode) using a Vibracell 600W (Sonics & Materials, Dantbury, CT). Droplets size of the resulting miniemulsion was measured immediately after sonication. The miniemulsion was then transferred to a Schlenk tube covered with a 3-way stopcock and purged with a little nitrogen flow during 45 min at 10°C. The reactor was then immersed in a thermostatted oil bath at 80°C to start polymerization. To determine conversion, molar masses and particles size, the resulting suspensions were divided in three parts. The first one was kept apart for size measurements. The second one was used to determine monomer conversion (x) by a gravimetric method after vacuum drying for 24 h. NCs were then washed twice with THF to extract free PMMA or poly(MMA-co-DEAEMA) chains not attached to dextran. These uncoupled grafts were analyzed by ^{1}H NMR in DMSO-d_6 (Figure S1) and SEC-MALLS in THF (Figure 2). The third part of the suspension was centrifuged. Recovered NCs were washed twice to extract non-reacted species and dispersed in deionized water for biological tests, whereas the floating was analyzed by anthrone titration [34] to estimate the quantity of $DexN_{3\text{-}20}CTA_{3.7}$ remaining in aqueous solution. By difference with the initially introduced amount, one can estimate the quantity of dextran derivative adsorbed at the NC surface.

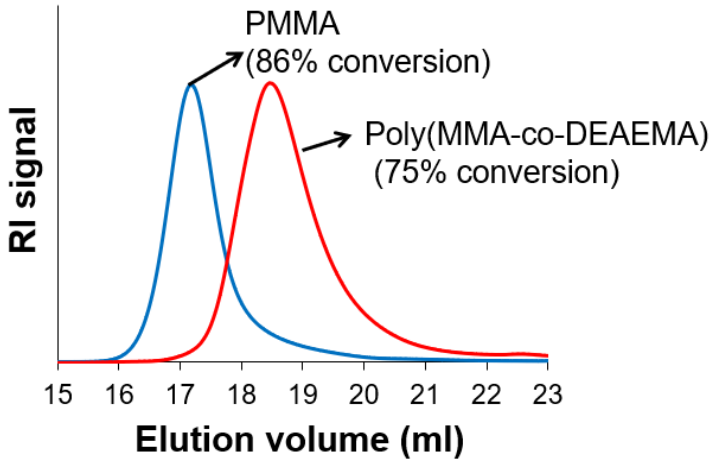

Figure 2. SEC traces of PMMA and poly(MMA-co-DEAEMA) free chains extracted with THF from the RAFT (co)polymerization in miniemulsion, at high conversion (Runs 1-2, Table 1).

2.3 Physico-chemical characterizations of NCs

^{1}H NMR spectra were recorded on a Bruker Avance 300 apparatus (300.13 MHz, 25°C) in DMSO-d_6. 1024 Scans were recorded.

SEC-MALLS analyses of PMMA and poly(MMA-co-DEAEMA) chains were performed in THF at 40^{o}C using a Waters 515 HPLC pump equipped with a degazer, a temperature controller and three PLgel 5µm columns (100 Å, 1000 Å and 10000 Å, columns (300 x 7.5 mm, P/N 1100-6350, Polymer laboratories)) at elution rate 1 mL/min. Two detectors were used online: a MALLS detector (Mini Dawn Treos Wyatt -Wyatt Technology Corporation) and a differential refractometer (OPTI Lab rex Wyatt). Solutions (10 mg/mL) were prepared by dissolution in the eluent and were left under vigorous stirring for 24 h. Filtration of these solutions was carried out right before injection. Refractive index increments (dn/dc) of 0.087 mL.g^{-1} and 0.10 mL.g^{-1} were used for PMMA and PDEAEMA in THF, respectively. dn/dc of poly(MMA-co-DEAEMA) was estimated by calculation using dn/dc of each homopolymer weighted by the weight fractions of each comonomer unit in the copolymers.

Droplet and NCs sizes were measured by a Dynamic Light Scattering (DLS) instrument (HPPS-ET, Malvern Instruments). Measurements were repeated three times and average values were given. The deviation remained below 5 %in all cases.

The electrophoretic mobility was measured in NaCl solutions of variable concentration (between 10^{-6} and 1 M) using a Zetasizer Nano-Z instrument (Malvern Instruments). Zeta potential (ζ) values were calculated from the electrophoretic mobility using the modified Booth equation [35] and then used to estimate the thickness of the dextran outer layer (Δ_{PZ}) by using the Eversole and Board equation as described in our previous works [36], [37].

2.4 Swelling measurements

The kinetics of swelling was studied by monitoring NCs size changes as a function of pH. NCs fresh suspension was diluted in 50 mL of PBS 0.148 M (1.4 mg NCs/mL). pH was fixed to 9 using NaOH 0.1 M and the suspension was split into 10 tubes (5 mL per tube). The pH in each tube was adjusted with HCl (0.1 M) to get pH values between 3 and 9. NCs average size was determined after 30 minutes of stirring. The pH of each sample was measured at the end of the experiment.

2.5 Cou1 *in vitro* release studies

Cou1-loaded NCs suspensions were diluted in 1 L of release media (PBS 0.148 M or PBS/SDS (0.148 M/1 wt.%), pH= 4 or 7.4) to a final concentration of 0.11 mg of NCs/mL. This suspension was maintained under magnetic stirring at 37°C and aliquots (2 mL) were withdrawn at different time points. NCs in each aliquot were removed by ultrafiltration using Millipore tubes (Ultrafree®-MC, 0,5 mL, PTFE, 0,2 µm). Cou1 release was monitored by fluorescence spectroscopy (Fluorolog-3, Jobin-Yvon Horiba S.A.S.). 0.5 mL of release media were mixed with 0.5 mL of ethanol and fluorescence emission was determined at 455 nm with an excitation peak wavelength of 372 nm. The Cou1 release amount was evaluated thanks to calibration curves (Figure S5).

2.6 Adsorption of proteins

NCs were dispersed in PBS (final concentrations ranging from 5.0×10^{-8} to 5.0×10^{-3} mg NCs /mL). Firstly, a set of NCs suspension was incubated for 24 h with the albumin solution (final concentration of 0.53 µM in PBS) at 37°C. Quenching of albumin fluorescence by NCs was monitored using a spectrofluorimeter (Hitachi F-2000, France) set at λ_{ex} 280 ± 10 nm, λ_{em} 350 ± 10 nm. Fluorescence intensities of albumin were recorded with (F) or without the NCs (Fo) as a function of the NCs concentrations. Then, a second set of NCs suspension was mixed with a fibrinogen solution (2 g/L in PBS), which was pre-warmed at 37°C for 10 min. After 2 h incubation at 37°C, the samples were centrifuged at 21 000 × *g* for 1 h. Then, 100 µL of supernatant was collected, diluted in PBS and fibrinogen quantification was performed using a microbicinchoninic acid test according to the manufacturer's specifications using a microplate reader (BioTeK EL 800).

2.7 *In vitro* cytotoxicity assays

Human non-adherent monocyte cells line, THP-1 (ATCC®, TIB-202™, Manassas, VA, USA) were cultivated in complete medium composed of RPMI 1640 medium supplemented with 10 % (v/v) of heat-inactivated fetal bovine serum, 100 U/mL of penicillin, 100 µg/mL of streptomycin, and 0.25 µg/mL of amphotericin B. Cells were grown at 37 °C under 5 % CO_2 atmosphere and split every 3 days.

Cells were seeded in 96-well plates at 125×10^3 cells per cm^2 and allowed to grown during 24 h at 37°C. Purified NCs suspension was diluted in PBS and then added onto cells to obtain final concentrations ranging from 5.0×10^{-8} to 5.0×10^{-3} mg NCs/mL (PBS alone was used as

control). After 24 h of incubation at 37°C, the metabolic activity of cells was determined with WST-1 assays performed according to manufacturer's protocol (Roche). This assay is based on the cleavage of a tetrazolium salt by cell mitochondrial deshydrogenase. The absorbance of the produced formazan salt was measured at 450 nm with reference wavelength of 620 nm. Numbers of dead and alive cells were also counted using the Trypan blue exclusion assay. Total cells count and percentage of viable and dead cells were determined with the automated cell counter (TC20, Biorad). Three independent batches of NCs, prepared under same polymerization conditions, were used in this study.

2.8 NCs surface post-functionalization

2.8.1 Grafting of Cou-click

A stock Cou-click solution was prepared by dissolving 10.4 mg in 8 mL of NaOH ($7x10^{-3}$M). 1 mL of this solution ($5.3x10^{-3}$ mmol of alkyne functions) was then mixed with 5 mL of NCs suspension (2.5 mg NCs/mL, 1.3 $x10^{-3}$ mmol of azide functions). After a 15 minutes degassing, 5 mg of CuBr (0.022 mmol) and 0.5 mg of Cu^{o} ($7.8x10^{-3}$ mmol) were added and the reaction was left to proceed under stirring during one day at room temperature. Reaction media was then treated with EDTA (5 equivalents/Cu) for 24 h. Cou-labelled NCs were recovered by centrifugation, washed twice and dispersed in deionized water. Fluorescence emission of Cou-click linked onto the NCs surface in water was determined at 432 nm with an excitation peak wavelength of 325 nm. A negative control was performed by mixing Cou-click and NCs without addition of copper catalyst.

2.8.2 Grafting of DBCO-PEG_4-TAMRA

A stock DBCO-PEG_4-TAMRA solution was prepared by dissolving 4.5 mg in 1 mL of DMSO. 0.4 mL of this solution (1.9 mmol of DBCO-PEG_4-TAMRA) were then mixed with 5 mL of NCs suspension (2.1 mg NCs/mL, 1.2 $x10^{-3}$ mmol of azide functions) and reaction was left to proceed under stirring during 30 min at room temperature. Labelled NCs were removed by ultrafiltration using Millipore tubes (Ultrafree®-MC, 0,5 mL, PTFE, 0,2 µm) and the resulting filtrate was analyzed by fluorescence spectroscopy. Fluorescence emission of the free DBCO-PEG_4-TAMRA was determined in water at 587 nm with an excitation peak wavelength of 545 nm. Number of DBCO-PEG_4-TAMRA molecules per NC was calculated as shown in supplementary information (Figure S7).

3. RESULTS AND DISCUSSION

Based on our previous researches [7], [8], [38], we selected Miglyol®810 (M810) as both co-stabilizer during the miniemulsion process and oily core of final NCs (Figure 1). M810 is a biocompatible triacylglycerol containing saturated fatty acids (mainly caprylic acid -69 wt%- and capric acid -30 wt%) and widely used in pharmaceutical formulations [39]. Furthermore, our objective was to use $DexN_3$-τCTAγ derivatives both as steric stabilizers and as macroCTA during polymerization. The surface activity of such $DexN_3$-τCTAγ has already been shown to be sufficient enough to stabilize water/(MMA+M810) interfaces under polymerization conditions (i.e. 80 °C, 3 h), when τ was higher than 18% [8]. The azide functions (N_3) located at the end of alkyl chains may be available at the surface of final NCs for post-functionalization with appropriate targeting ligands, thus extending the range of applications of these nanocarriers (e.g. diagnostics, cancer cells specific targeting…). Dithiobenzoate CTA have also been grafted on dextran to provide a good control of RAFT miniemulsion polymerization of MMA at water/(MMA+M810) interface [8]. By this way PMMA-grafted dextran copolymers were produced at the interface leading to dextran coverage/PMMA shell/oily core NCs having various M810 contents and a well-defined PMMA (i.e. $Đ < 1.2$) shell (Figure 1). We were expecting that these CTA groups were also appropriate for RAFT miniemulsion copolymerization of MMA with DEAEMA. Indeed, RAFT homogeneous homopolymerization of DEAEMA has been successfully performed in ethanol [26], [40] or in 1,4-dioxane [14], [41] using 4-cyanopentanoic acid dithiobenzoate (CPADB) as molecular CTA. In addition, RAFT copolymerizations of DEAEMA with 2-(dimethylamino)ethyl methacrylate [24] or 2-(diisopropylamino)ethyl methacrylate [14] have also been reported in 1,4-dioxane using 2-cyanoprop-2-yl dithiobenzoate (CPDB) and CPADB, respectively. Both CPDB and CPADB are dithiobenzoate CTAs having a similar structure to the CTA groups introduced on the dextran-based transurf. Based on our previous work [8], we focused in this study on $DexN_{3\text{-}20}CTA_{3.7}$ transurf, having 20 N_3-end alkyl chains and 3.7 CTA groups per 100 glucopyranosic units.

3.1 RAFT miniemulsion (co)polymerization

Miniemulsions were initially obtained by mixing monomer(s) (MMA or MMA/DEAEMA mixture) and M810 together with AIBN, and then emulsifying the mixture in an aqueous solution containing 10 g/L of $DexN_{3\text{-}20}CTA_{3.7}$. $DexN_{3\text{-}20}CTA_{3.7}$ as stabilizer was initially adsorbed at the (monomer(s)+M810)/water interface. As macroCTA, the dithiobenzoate groups

mediated RAFT polymerization, producing polymeric grafts anchored to the dextran chains via the R-group approach. At the end, NCs having dextran outer surface covalently linked to the polymeric shell were produced (Figure 1). In the initial miniemulsion, monomer(s) were miscible with M810 but phase separation occurred during polymerization because of the immiscibility of the (co)polymer grafts with M810. Herein, a large amount of M810 (about 25-30% v/v to monomers) was used to favor such core-shell structure. Indeed, M810 segregation was evidenced by the presence of M810 fusion pic at about -5 °C on MDSC thermograms of final nano-objects (Figure S2) as we already observed in case of PMMA-NCs [8]. Depending on the miniemulsion recipe, the M810 oily core of NCs was surrounded by either a PMMA or a poly(MMA-co-DEAEMA) shell (Runs 1-2, Table 1.). These objects were named PMMA-NCs and COPO-NCs, correspondingly.

The amount of $DexN_{3\text{-}20}CTA_{3.7}$ linked at NCs surface was indirectly deduced by titration of the surfactant remaining in the aqueous phase after particle removal, following the anthrone method, and expressed as a percentage of the initially introduced amount. We assumed here that this amount corresponded to the $DexN_{3\text{-}20}CTA_{3.7}$ initially adsorbed at the monomer droplet interface as it became quickly irreversibly anchored at the interface thanks to the polymer grafts propagation. 94% and 90% of the transurf was found to be located at the interface of MMA and MMA/DEAEMA miniemulsions respectively, which is perfectly coherent with our previous results [7], [8]. These high values helped to prevent homogenous nucleation during the process which is convenient to control the NCs morphology. Knowing the amount of transurf at the nanodroplets interface, as well as the total amount of monomer(s) in the system, it was possible to calculate the initial $[DEAEMA]_o/[CTA]_o$ and/or $[MMA]_o/[CTA]_o$ molar ratios at the droplet interface. In the case of MMA homopolymerization, $[MMA]_o/[CTA]_o/[AIBN]_o$ was chosen equal to 393/1/0.3 as the polymerization control was already optimized with such conditions [8].

DEAEMA has lower water solubility in basic medium because of its protonable amine groups (pK_a = 8.6) [42]. However, ester linkages between both hydrophobic chain and CTA groups and dextran are prone to undergo hydrolysis in such basic conditions. Consequently, we imagined the polymerization could not be carried out in basic media ensuring the hydrophobicity of DEAEMA. To confirm this hypothesis, a preliminary assay was performed by stirring $DexN_{3\text{-}20}CTA_0$ (without CTA group) during 3 h. at 80 °C in aqueous basic media (pH=10). Only 25% of hydrophobic groups remained attached to dextran. As a result, surfactant properties of $DexN_{3\text{-}20}CTA_0$ would diminished and miniemulsion stability would be lost during polymerization.

Miniemulsion copolymerization was therefore carried out in pure water and an excess of DEAEMA was added to compensate the amount of monomer remaining in the aqueous phase (DEAEMA water solubility was estimated at 67 g/L). $[MMA]_o/[DEAEMA]_o/[CTA]_o/[AIBN]_o$ molar ratios in initial nanodroplets were equal to 115/120/1/0.3.

Table 1. RAFT homopolymerization (MMA) and copolymerization (MMA/DEAEMA) carried out from $DexN_{3\text{-}20}CTA_{3.7}$ in miniemulsion. Grafts characterization, loading efficiency and NCs size.

Run	NCs	Conv (%)[(a)]	Cou1 EE(%)[(b)]	Cou1 load (wt%)[(c)]	Final NCs diameter (nm)[(d)]	F_{DEAEMA}		$\bar{M}_{n\,Th}$[(f)] (g/mol)	dn/dc [(g)]	$\bar{M}_{n\,exp}$[(h)] (g/mol)	Đ[(h)]
						In feed	In copolymer[(e)]				
1	PMMA	86	-	-	119 ± 4 (0.21)	0	0	33 400	0.087	54 700	1.16
2	COPO	75	-	-	195 ± 10 (0.14)	0.66	0.75	25 400	0.097	41 400	1.09
3	PMMA	90	99	1.4	117 ± 5 (0.22)	0	0	35 400	0.087	54 500	1.18
4	COPO	78	99	1.7	198 ± 9 (0.15)	0.66	0.79	26 700	0.097	43 100	1.08

COPO is the abbreviation for Poly(MMA-co-DEAEMA). All experiments were carried out at 80 °C, 3 h, $[DexN_{3\text{-}20}CTA_{3.7}]$ = 10 g/L. $[MMA]_o/[DEAEMA]_o/[CTA]_o/[AIBN]_o$ molar ratios in initial nanodroplets were equal to 393/0/1/0.3 and 115/120/1/0.3 for PMMA-NCs and COPO-NCs, respectively. M810/monomers ratio was equal to 25 vol% and 30 vol% for PMMA-NCs and COPO-NCs, respectively. For runs 3 and 4, Cou1 was added into the organic phase at 76 mg per mL of M810.

(a) Monomer(s) conversion estimated by gravimetry.

(b) Cou1 loading efficiency indirectly determined by fluorescence quantification of Cou1 lost in the aqueous phase during encapsulation process. Verified by NMR ^1H spectrum of NCs in case of PMMA-NCs.

(c) Weight content of Cou1 inside NCs.

(d) Sizes were measured by DLS (n=3) and values under brackets correspond to PDI.

(e) DEAEMA weight fraction in copolymer grafts (see Figure S1).

(f) Theoretical molecular weight of grafts based on conversion and estimated by the following equation: $\bar{M}_{n\,Th} = \frac{[MMA]_0}{[CTA]_0} M_{MMA} x_{MMA} + \frac{[DEAEMA]_0}{[CTA]_0} M_{DEAEMA} x_{DEAEMA,}$ where x_{MMA} and x_{DEAEMA} are comonomer conversions.

(g) dn/dc value of poly(MMA-co-DEAEMA) in THF estimated by the following equation $(dn/dc)_{copolymer} = F_{PDEAEMA}\,(dn/dc)_{PDEAEMA} + (1- F_{PDEAEMA})\,(dn/dc)_{PMMA}$, where $(dn/dc)_{PDEAEMA}$ = 0.10 and $(dn/dc)_{PMMA}$= 0.087.

(h) *Evaluated by SEC-MALLS in THF of free PMMA or poly(MMA-co-DEAEMA) chains extracted with THF from the final NCs, with dn/dc calculated in (g).*

According to the RAFT mechanism [43], grafts growing from CTA groups of $DexN_{3\text{-}20}CTA_{3.7}$ at the nanodroplets interface are in a dynamic equilibrium with the non-grafted chains (also called free chains) issued from AIBN-derived radicals and propagating inside the droplets, as we previously reported in the case of MMA RAFT polymerization [8]. These free chains have similar composition and length than the grafts linked to dextran. Therefore, the low amount of free chains formed in the organic phase could be used to approximate molecular weight, molecular weight distribution and composition of grafted polymers. Figure 2 shows SEC traces of free PMMA and poly(MMA-co-DEAEMA) chains extracted with THF from the polymerization mixtures at high conversion. The monomodal and very narrow molecular weight distributions are further evidences for control of the RAFT polymerization (Table 1). In the case of COPO-NCs, both monomers MMA and DEAEMA were expected to be statistically distributed along the polymeric chains as indicated by the reactivity ratios obtained for free radical bulk copolymerizations performed at 60°C (r_{DEAEMA}=1.27 and r_{MMA}=0.89) [44]. DEAEMA content of poly(MMA-co-DEAEMA) free chains was estimated using ^{1}H NMR spectroscopy (Figure S1). DEAEMA weight fraction (F_{DEAEMA}) could be evaluated at 0.75 at a global conversion of 75%. Thanks to this value, the dn/dc of the copolymer could be calculated and subsequently $\bar{M}_n$ was evaluated by SEC-MALLS ($\bar{M}_{n\,exp}$, Table 1.). As shown (Runs 1-2, Table 1), $\bar{M}_{n\,exp}$ were much higher compared to theoretical ones ($\bar{M}_{n\ Th}$). As previously reported [8], the poor accessibility of some CTA groups towards organic phase reduces their efficiency, thus increasing the degree of polymerization of grafts at the same conversion. For MMA RAFT polymerization using $DexN_{3\text{-}20}CTA_{3.7}$ as transurf, the efficiency of reactive groups was formerly estimated at 50% [8]. This efficiency seemed to be comparable in the case of MMA/DEAEMA copolymerization.

In conclusion, these first assays confirmed the possibility to mediate RAFT miniemulsion copolymerization of MMA with DEAEMA from a multifunctional polysaccharide transurf in order to prepare dextran-covered oily core NCs with a poly(MMA-co-DEAEMA) internal shell, which is potentially pH-responsive.

3.2 NCs characterization

COPO-NCs final size (about 195 nm) was higher than PMMA-NCs one (about 119 nm) in agreement with the less hydrophobic character of the poly(MMA-co-DEAEMA) shell and the more polar nature of DEAEMA monomer. Monomodal and narrow distributions were observed

in both cases. Evaluation of NCs zeta potential as a function of ionic strength allowed us to evidence the presence of a dextran outer shell onto NCs surface and to estimate its thickness (Δ_{PZ}). Δ_{PZ} has been evaluated at 5 nm for both PMMA-NCs and COPO-NCs. Moreover, a very low zeta potential value (i.e. an almost neutral surface) was observed for both kinds of particles at the ionic concentration of human blood plasma (0.148 M). The stability of the NCs has been as well examined by turbidimetry in saline solutions at various ionic strengths (ranging from 10^{-5} to 2 M) (Figure S3). Accordingly, NCs should display a convenient stability in physiological media. The dextran shell stability due to the covalent linkage between dextran chains and NCs shell (thanks to CTA groups of $DexN_3$-τCTAγ) was also assessed using a drastic anionic surfactant, sodium dodecyl sulfate (SDS, Figure S4). Consequently, this should favor the stability of dextran coverage upon intravenous injection as circulating proteins like opsonins could act as SDS.

3.3 Biomedical potential

3.3.1 pH-sensitivity of COPO-NCs

Because of their high glycolytic rates, cancer cells exhibit an acidic environment (pH around 6.5) whereas physiological blood pH remains constant at 7.4 [12]. In addition, lower pH values are found in intracellular organelles such as endosomes (pH between 5 and 6) and lysosomes (pH around 4.5) [10, 47, 48]. Therefore an ideal drug pH-sensitive nanocarrier is expected to protect and keep the drug at normal pH and release it under weakly acidic conditions [47].

With the aim of studying the response of PMMA-NCs and smart COPO-NCs to pH variations, the hydrodynamic diameters of these NCs were measured at different pH values and at 25 °C by DLS. In order to be as close as possible to real physiological conditions, PMMA-NCs and COPO-NCs were dispersed in phosphate buffered saline (PBS) at the ionic strength of human blood (0.148 M). In both cases, pH was first set in the basic range (9-10) adding NaOH and progressively decreased down with HCl. Results are summarized in Figure 3.

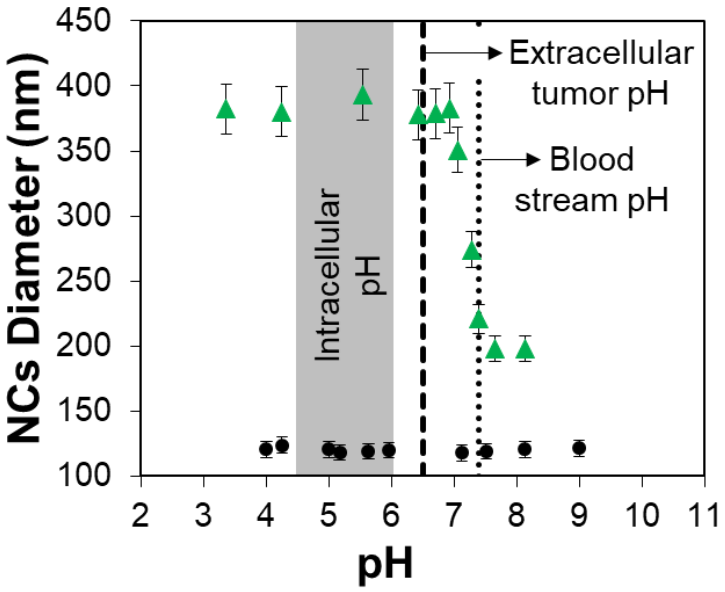

Figure 3. pH-responsive swelling of NCs. Average hydrodynamic NCs diameter (determined by DLS) as a function of pH at 25 °C in PBS-0.148M: (●) PMMA-NCs and (▲) COPO-NCs.

As expected, PMMA-NCs exhibited no swelling in aqueous PBS buffers having pH from 3 to 9. To the contrary, COPO-NCs exhibited a 2-fold change in diameter in PBS buffer by changing the pH from the blood stream (pH = 7.4) to the internal tumor cells (pH from 4 to 6). Based on this diameter variation, a volume increase of more than 7 times could be estimated. This transition resulted from the protonation (in acidic media) of the amine groups of DEAEMA units in the grafts constituting the polymeric shell [32]. Electrostatic repulsions between protonated groups resulted in swelling of NCs shell. Swelling transition was detected at pH ~ 7.4 in PBS (0.148 M) (Figure 3). According to these results, pH-sensitive COPO-NCs could be potentially interesting drug delivery systems for *in vivo* cancer therapy. Nevertheless, the shell composition should be optimized (variation of MMA/DEAEMA ratio [48] or of pH-sensitive co-monomer [49]) to reach a swelling transition around 6.5 in order to avoid a low premature drug release during blood circulation and to get a rapid drug discharge after reaching tumor tissues.

3.3.2 Loading and release studies

In order to study the pH-responsive drug release properties of PMMA-NCs and COPO-NCs, a fluorescent model dye (7-diethylamino-4-methylcoumarin, Cou1, Figure 4) was chosen. In a typical loading experiment, Cou1 was added into the organic phase at a constant concentration (76 mg per mL of M810), which was below the maximum solubility of Cou1 in this oil

(estimated at 92 mg/mL). Cou1 encapsulation was achieved in one-pot during the NCs production. As shown in Table 1, Cou1 could be efficiently loaded into both PMMA-NCs (Run 3, Table 1) and COPO-NCs (Run 4, Table 1) with high encapsulation efficiency (99%). Cou1 loading was found to be 14 mg/g of PMMA-NCs (1.4 wt%) and 17 mg/g of COPO-NCs (1.7 wt%) as shown in Table 1. The efficient Cou1 encapsulation was most likely due to its very low solubility in water pH=6.8 (estimated at 0.026 mg/ml by fluorescence spectroscopy) that limited its diffusion into the aqueous phase during polymerization or washing steps. NCs final sizes as well as polymer shell macromolecular parameters were similar with those observed for non-loaded PMMA-NCs (Run 3 vs Run 1, Table 1) and COPO-NCs (Run 4 vs Run 2, Table 1). This suggested that Cou1 has no influence on RAFT polymerization nor on miniemulsion stability.

The pH-dependent release profile of Cou1 from PMMA-NCs has been firstly investigated *in vitro* by monitoring Cou1 release in PBS (0.148 M) under physiological (pH = 7.4) and acidic conditions (pH = 4.0) (Figure 4). Cou1 solubility in PBS was evaluated by fluorescence spectroscopy to be about 0.023 mg/mL and 0.031 mg/mL at pH 7.4 and 4, respectively. Cou1-loaded NCs concentration in release media was in consequence fixed to about 100 mg NCs/L in order to assure perfect sink conditions. Release studies were performed in a batch sealed system maintained at 37°C and samples were taken at different times without refreshing of dissolution medium. The relative amount of released Cou1 was estimated by fluorescence spectroscopy of the dissolution media after NCs removal.

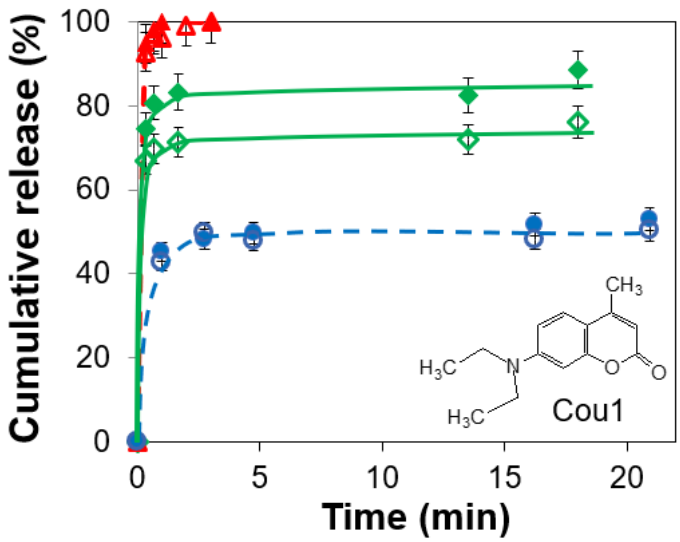

Figure 4. pH-triggered release of Cou1 at 37°C from PMMA-NCs in (●) PBS (Run 3, Table 1) or (▲) PBS/SDS (Run 3, Table 1) and from COPO-NCs in (♦) PBS (Run 4, Table 1). Full symbols (pH = 4.0) and open symbols (pH= 7.4).

Whatever the pH value (4 or 7.4) is, only 50% of Cou1 was released from PMMA-NCs (Run 3, Table 1) in PBS buffer within the first 20 minutes and no further release was observed during the next 22 h. This supported the fact that PMMA-NCs are stable under acidic conditions with no influence of pH. Furthermore, since Cou1 solubility was not highly sensitive to pH, similar release profiles were expected at both pH conditions. Two more release tests were then performed with Cou1-loaded PMMA-NCs (Run 3, Table 1) in PBS buffer containing 1 wt% of SDS (PBS/SDS) as release medium. SDS was added above its critical micelle concentration (CMC~0.23wt% in water and ~0.06wt% in PBS (0,05M pH = 7,0)) [50] to ensure the formation of surfactant micelles able to further solubilize released Cou1. When compared to the PBS solution and whatever the pH value, PBS/SDS micellar solution resulted in an 80-fold increase of Cou1 solubility (estimated by fluorescence spectroscopy at about 2.0 mg/mL and 2.3 mg/mL at pH 7.4 and 4, respectively). Cou1 release was therefore favored in these last conditions and completely achieved within 1 hour independently of the pH of the dissolution media (Figure 4). This proved that the previous partial release of Cou1 in PBS was not due to secondary reactions preventing the effective and total Cou1 delivery. Indeed, when comparing these last results (in PBS/SDS) with former ones (PBS), Cou1 release seemed to be mainly driven by its partition coefficient between the oily core of NCs and the aqueous external media rather than by its diffusion through the polymeric membrane shell as it should be expected for sink conditions.

Regarding COPO-NCs (Run 4, table 1), Cou1 delivery profiles with similar shape were obtained at both pH in PBS buffer but Cou1 release was increased (12% net difference) in acidic media (Figure 4). These results were consistent with the previous pH-response studies (see section 3.3.1) wherein the maximal swelling ratio of COPO-NCs was found for pH values below 6, while collapsed state was observed at pH 7.4 or above. Consequently, Cou1 dissolution into the aqueous media was thus enhanced in acidic conditions by the hydration of the poly(MMA-co-DEAEMA) shell and its increased permeability.

When comparing PMMA-NCs and COPO-NCs release studies in PBS buffer at physiological pH, the release rate of Cou1 was faster through the poly(MMA-co-DEAEMA) shell with 70% of Cou1 being delivered within 20 minutes whereas 50% was only released from PMMA-NCS in the same time. This difference probably arises from the unlike chemical nature of NCs internal shell but certainly more from morphological differences between both NCs types: at physiological normal pH, COPO-NCs were slightly swollen compared to PMMA-NCs as shown in Figure 3 thereby further enhancing Cou1 diffusivity.

In summary, these studies demonstrated the potential of PMMA-NCS and COPO-NCs to be used as reservoirs of hydrophobic drugs. Despite, some optimization may be required to get a well-controlled and sustained drug release under physiological ionic strength and pH variations (i.e. drug retention in blood circulation and release in tumor cells). Varying DEAEMA content and/or crosslinking of poly(MMA-co-DEAEMA) shell in COPO-NCs could be suitable approaches for fine-tuning of their pH-sensitive properties and for decreasing premature load release.

3.3.3 Interaction with blood proteins

It is well known that interaction of DDS with blood components (i.e blood cells, proteins, lipoproteins…) may modify DDS surface properties and determine their *in vivo* outcome [51]. As first assessment, the PMMA-NCs and COPO-NCs interactions with blood proteins were studied to check whether albumin (the most important plasmatic protein in quantity) and fibrinogen (a key protein for coagulation) were adsorbed on NCs surface. Albumin fluorescence quenching is a classical approach to study its adsorption on DDS surface [52], [53]. Whatever the tested NCs (Cou1 unloaded), no difference in term of fluorescence intensities of albumin was measured in presence or in absence of NCs (Figure 5a). Moreover, a total recovery of the initial fibrinogen concentration was observed after NCs incubation (Figure 5b). These results showed an absence of protein adsorption on NCs surface due to hydrophilic dextran corona around the hydrophobic PMMA or poly(MMA-co-DEAEMA) internal shell. Dextran outer layer is expected to provide a stealth surface coating allowing an improved NCs circulation lifetime, at least enough to ensure their recognition by pathological cells in the case of an active targeting strategy.

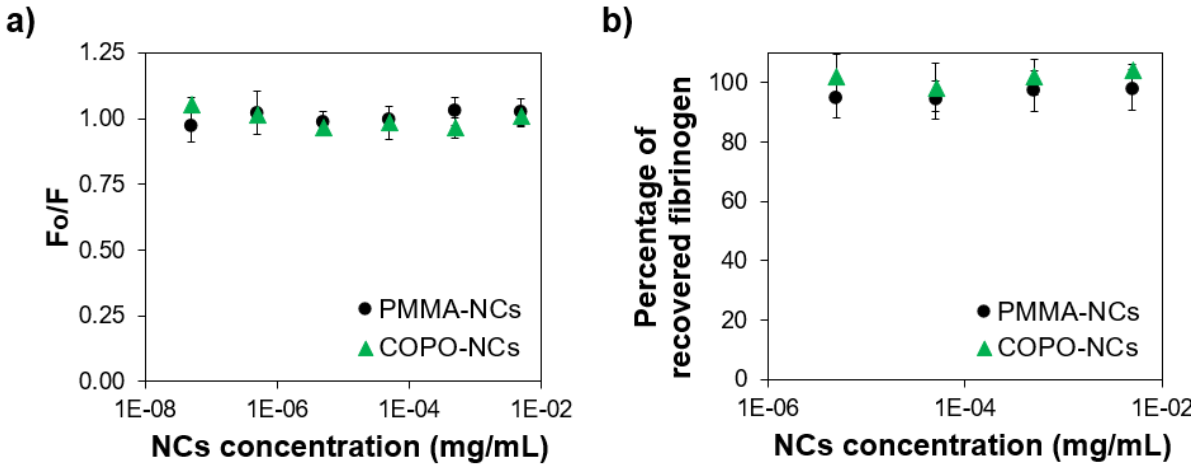

Figure 5. a) BSA fluorescence intensities in presence (F) or in absence (Fo) of NCs (without Cou1 loading) and b) percentage of fibrinogen recovered after incubation of NCs (table 1), n=3.

3.3.4 NCs cytotoxicity

Whatever the studied DDS, an additional concern is their own potential toxicity. PMMA-NCs and COPO-NCs (Cou1 unloaded) were thus incubated with monocytes (THP-1) and showed no cytotoxicity regarding to the Trypan blue assay as more than 96 % of viable cells were observed whatever the NCs concentration was. Then, the metabolic activity of THP-1 cells through the cleavage of tetrazolium salt by mitochondrial deshydrogenase was evaluated to more than 90 % of the control one. Consequently, both PMMA-NCS and COPO-NCs were found cytocompatible (Figure 6a). As metabolic activity is also a function of cells number, the ratio between absorbance of formazan salt produced and the number of living cells was calculated. As shown in Figure 6b, none of the conditions were different from the control proving that PMMA-NCS and COPO-NCs did not influence cells viability nor proliferation of THP-1, and could be considered as cytocompatible.

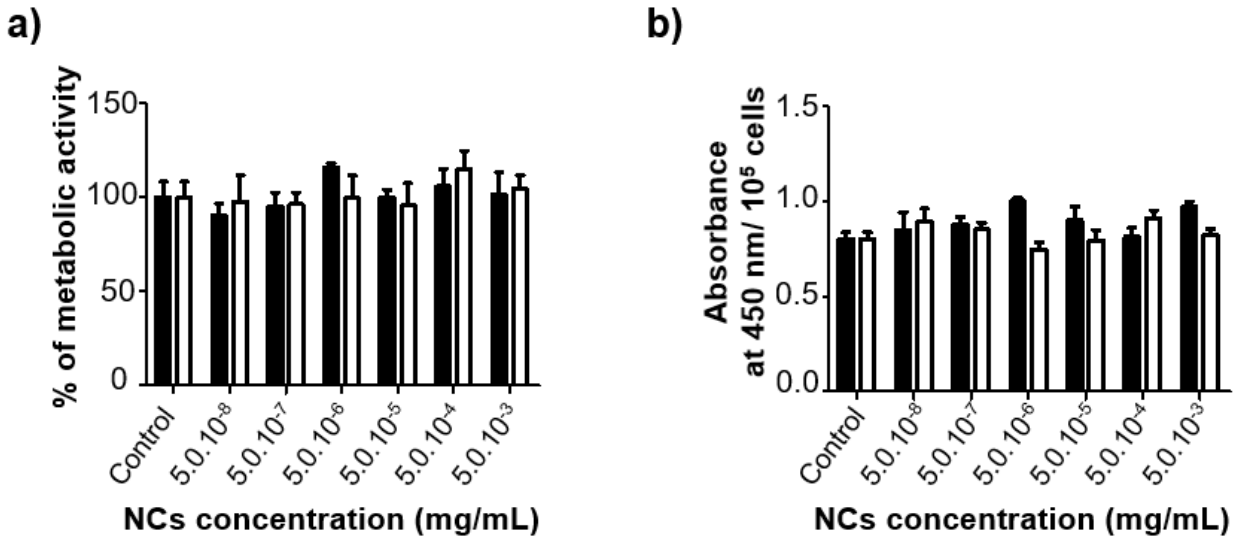

Figure 6. Cytocompatibility of unloaded PMMA-NCS (in black) or COPO-NCs (in white) incubated in PBS during 24 h at 37°C with human monocytes (THP-1). a) Metabolic activity (WST-1 assay). b) Ratio of the metabolic activity (WST-1 absorbance at 450 nm) and the number of living cells determined by the Trypan blue assay. Results are expressed as mean ± standard error of the mean, n = 3.

3.3.5 NCs surface labeling

One strategy for cells specific targeting involves the grafting of active targeting ligands on DDS surface that are able to bind to tumor tissues [3]. As mentioned before, dextran coverage of NCs

was deliberately decorated with free azide functions located at the end of alkyl chains with the aim to allow facile post-functionalization chemistry (Figure 1). Surface modification feasibility was evaluated by grafting of fluorescent molecules onto PMMA-NCs *via* two approaches (Figure 7): i) a Cu (I)-catalyzed click-chemistry reaction with the end-alkyne groups of Cou-click and ii) a Cu-free click-chemistry reaction with the cyclooctyne group of DBCO-PEG_4-TAMRA.

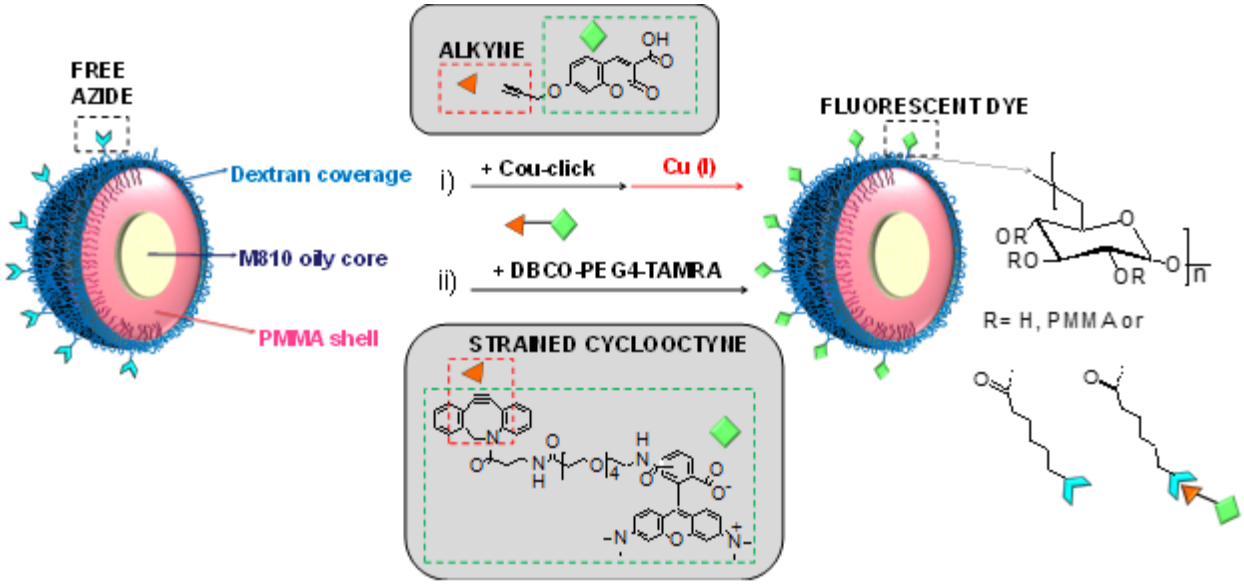

Figure 7. NCs post-functionalization strategies by click chemistry.

In the former case, a classical Cu-catalyzed click reaction was performed. Cou-click was added in a 4-fold excess over free azide groups and the reaction was carried out during 24 h. at room temperature after addition of copper catalyst. In parallel, a blank sample containing NCs and Cou-click without any catalyst was also prepared and maintained 24 h. under magnetic stirring. The presence of grafted dye at NCs surface (when adding copper catalyst) was checked by fluorescence spectroscopy (Figure S6b). Slight difference in emission was observed between initial NCs (before click reaction) and blank NCs (no catalyst). This could be ascribed to Cou-click traces still present after NCs purification. Nevertheless, purified cou-labeled PMMA-NCs exhibited a clear and much bigger peak at 432 nm in the fluorescence spectrum when excited at 325 nm in water. This peak was assignable to grafted Cou-click as corresponding to emission range of pure dye (Figure S6a). These observations confirmed both the feasibility of such NCs surface modification, the need of a copper catalyst to carry out the reaction and that Cou-click was covalently bound to dextran coverage and not just adsorbed on NCs surface. The presence of outer free azide functions available for reaction at the NCs surface was as well evidenced. To

prevent the probable distortion of the measured emission values by copper catalyst, the Cou-labelled PMMA-NCs were purified by adding ethylenediaminetetraacetic acid as copper complexing agent followed by several washings with water. Such a treatment was expected to take off more than 99% of copper and then to reduce the copper amount to a very low concentration (less than 150 ppm) as already observed in our previous works [36, 37]. However, the comparison of fluorescence emission measurements of Cou-labelled NCs with a standard curve of pure Cou-click mixed with non-modified NCs in aqueous phase lead to an overestimation of the grafted dye. Thus, only a qualitative assessment of click-reaction was possible. An explanation is that fluorescence properties of Cou-click covalently linked to NCs are quite different of those of molecular fluorescent dye, maybe due to triazole ring formation.

For the second coupling assay, Cu(I)-free or strain promoted click chemistry reaction was performed with cyclooctyne groups of DBCO-PEG_4-TAMRA. DBCO-PEG_4-TAMRA is an azide-reactive fluorescent dye commonly used for labeling and visualizing chemically azide-modified biomolecules *in vivo* (e.g. peptides) without observable cytotoxicity [54]. Cyclooctyne in DBCO part reacts with azide at room temperature without the need of a copper catalyst and produces a stable triazole [55]. Consequently, reactions using cyclooctynes are more suitable in biomedical field as overcoming the intrinsic toxicity of copper catalyst [56]. Herein, the reaction was performed during 30 minutes with a 2-fold excess of cyclooctyne groups over free azide functions of NCs. The functionalization of PMMA-NCs was confirmed in both qualitatively and quantitatively fashions. After reaction and several washings, the initially white PMMA-NCs suspension turned into a dark pink color attesting DBCO-PEG_4-TAMRA grafting (Figure 8). The amount of grafted dye was indirectly determined by fluorescence titration of DBCO-PEG_4-TAMRA remaining in the aqueous phase after NCs centrifugation and removal. Emission fluorescence was converted to DBCO-PEG_4-TAMRA concentration thanks to a calibration curve of pure DBCO-PEG_4-TAMRA in water. The yield of click-chemistry was estimated to be 25%, which meant that 25 per 100 of the azide functions of dextran coverage have been reacted during this reaction time. This corresponded to about 12 000 DBCO-PEG_4-TAMRA molecules per NC. This showed the potential to use those NCs surface azide functionality to covalently attach targeting ligands showing specificity for cancer cells in the future.

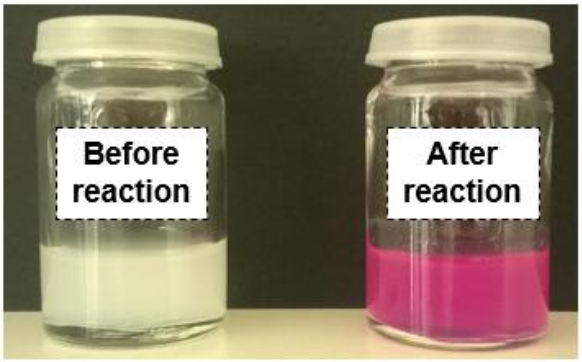

Figure 8. Copper-free click chemistry between DBCO-PEG$_4$-TAMRA and free azide functions of dextran coverage. PMMA-NCs dispersions prior and after click reaction.

CONCLUSIONS

The use of a multifunctional transurf based on dextran in a RAFT miniemulsion polymerization was investigated to produce for the first smart oily core NCs. Those NCs with both pH-sensitive shell and functionalizable dextran- surface have been designed in view of potential anti-cancer drug delivery systems.In addition to the challenge to perform RAFT polymerization of DEAEMA in heterogenous conditions, considering its partial solubility in water, the control of the dextran-covered NCs morphology was remarkably achieved by confining the polymerization at the droplet interface of the direct miniemulsion thanks to the use of a multi-reactive dextran-based transurf. Our previous works on MMA homopolymerization [7,8] were successfully extended to MMA/DEAEMA copolymerization allowing the incorporation of DEAEMA in the NCs internal shell. Both PMMA and poly(MMA-co-DEAEMA)-based NCs were further characterized regarding on their potential for biomedical applications, particularly in view of cancer treatment. The *in vitro* assays we performed on the basis of previous works [51, 52, 53] depicted promising properties of these objects for intravenous administration: i) size about 100 nm, ii) almost neutral surface and good colloidal stability at physiological ionic strength, iii) very stable hydrophilic dextran coverage providing protection against non-specific interactions with plasmatic proteins (BSA and fibrinogen) iv) potential oily reservoirs for hydrophobic drugs and v) no cytotoxicity to human monocyte. In addition, both PMMA-NCs and COPO-NCs were evaluated for the encapsulation of a model hydrophobic active substance (Cou 1) and a high loading efficiency (99 %) was obtained. During Cou1 release experiences, we demonstrated that poly(MMA-co-DEAEMA) shell of COPO-NCs presented pH sensitivity in the physiologically relevant pH range, thus allowing a pH-tunable Cou1 release behavior. Preliminary assays to bind

fluorescent dyes on NCs surface showed promising results: a large amount of the azide functions of the dextran-based transurf was effectively available for click post-functionalization. This gave the possibility to attach targeting moieties to enhance NCs uptake by tumor cells. Overall, this work highlighted the value of this NCs platform for potential *in vivo* cancer drug delivery. Nevertheless, the shell composition should be optimized to reach a swelling transition around pH=6.5. Commonly used, *in vitro* blood compatibility tests like complement activation will be applied in the near future in order to get further information on NCs suitability to be injected as DDS. NCs loaded with different anticancer agents could be as well prepared. After functionalization with the appropriate(s) ligands, such NCs could be used to target a particular cancer pathology.

CRediT author statement:

Laura Marcela Forero Ramirez: Investigation, Data curation, Visualization. Writing - Original Draft. **Ariane Boudier**: Visualization, Writing - Review & Editing. **Caroline Gaucher** Visualization, Writing - Review & Editing. **J. Babin** Visualization. **Alain Durand** Visualization. **J-L. Six**: Supervision, Validation, Review & Editing. **C. Nouvel**: Conceptualization, Methodology, Project administration, Funding acquisition, Validation, Supervision, Writing - Review & Editing

Acknowledgments

The authors express their highest gratitude to Marie-Christine Grassiot for help in SEC measurements, to Olivier Fabre for NMR measurements, to Isabelle Fries for cytotoxicity assays and to the physicochemical platform of the Faculty of Pharmacie (Nancy-France) for help in protein-NCs interactions analyses. C. Nouvel and L.M Forero Ramirez acknowledge support from ANR JCJC ANR-12-JS08-0003-01 NANOCAPDEX for funding and PhD Research Fellowship, respectively.

REFERENCES

[1] C. E. Wang, P. S. Stayton, S. H. Pun, et A. J. Convertine, « Polymer nanostructures synthesized by controlled living polymerization for tumor-targeted drug delivery », *Journal of Controlled Release*, vol. 219, p. 345‑354, déc. 2015.
[2] C. M. Dawidczyk *et al.*, « State-of-the-art in design rules for drug delivery platforms: Lessons learned from FDA-approved nanomedicines », *Journal of Controlled Release*, vol. 187, p. 133‑144, août 2014.
[3] A. Wicki, D. Witzigmann, V. Balasubramanian, et J. Huwyler, « Nanomedicine in cancer therapy: Challenges, opportunities, and clinical applications », *Journal of Controlled Release*, vol. 200, p. 138‑157, févr. 2015.
[4] N. A. Fonseca, A. C. Gregório, Â. Valério-Fernandes, S. Simões, et J. N. Moreira, « Bridging cancer biology and the patients' needs with nanotechnology-based approaches », *Cancer Treatment Reviews*, vol. 40, n° 5, p. 626‑635, juin 2014.
[5] C. Lemarchand, R. Gref, et P. Couvreur, « Polysaccharide-decorated nanoparticles », *European Journal of Pharmaceutics and Biopharmaceutics*, vol. 58, n° 2, p. 327‑341, sept. 2004.
[6] C. Lemarchand *et al.*, « Influence of polysaccharide coating on the interactions of nanoparticles with biological systems », *Biomaterials*, vol. 27, n° 1, p. 108‑118, janv. 2006.
[7] L. M. Forero Ramirez, J. Babin, M. Schmutz, A. Durand, J.-L. Six, et C. Nouvel, « Multi-reactive surfactant and miniemulsion Atom Transfer Radical Polymerization: An elegant controlled one-step way to obtain dextran-covered nanocapsules », *European Polymer Journal*, vol. 109, p. 317‑325, déc. 2018.
[8] L. M. Forero Ramirez *et al.*, « First multi-reactive polysaccharide-based transurf to produce potentially biocompatible dextran-covered nanocapsules », *Carbohydrate Polymers*, vol. 224, p. 115153, nov. 2019.
[9] S. Mura, J. Nicolas, et P. Couvreur, « Stimuli-responsive nanocarriers for drug delivery », *Nature Materials*, vol. 12, n° 11, p. 991‑1003, oct. 2013.
[10] M. El Founi *et al.*, « Light-sensitive dextran-covered PNBA nanoparticles as triggered drug delivery systems: Formulation, characteristics and cytotoxicity », *Journal of Colloid and Interface Science*, vol. 514, p. 289‑298, mars 2018.
[11] J. I. Amalvy, E. J. Wanless, Y. Li, V. Michailidou, S. P. Armes, et Y. Duccini, « Synthesis and Characterization of Novel pH-Responsive Microgels Based on Tertiary Amine Methacrylates », *Langmuir*, vol. 20, n° 21, p. 8992‑8999, oct. 2004.
[12] J. Liu *et al.*, « pH-Sensitive nano-systems for drug delivery in cancer therapy », *Biotechnology Advances*, vol. 32, n° 4, p. 693‑710, juill. 2014.
[13] L. Liu *et al.*, « Controlled polymerization of 2-(diethylamino)ethyl methacrylate and its block copolymer withN-isopropylacrylamide by RAFT polymerization », *Journal of Polymer Science Part A: Polymer Chemistry*, vol. 46, n° 10, p. 3294‑3305, mai 2008.
[14] Y. Q. Hu, M. S. Kim, B. S. Kim, et D. S. Lee, « RAFT synthesis of amphiphilic (A-ran-B)-b-C diblock copolymers with tunable pH-sensitivity », *Journal of Polymer Science Part A: Polymer Chemistry*, vol. 46, n° 11, p. 3740‑3748, juin 2008.
[15] S. Yusa, M. Sugahara, T. Endo, et Y. Morishima, « Preparation and Characterization of a pH-Responsive Nanogel Based on a Photo-Cross-Linked Micelle Formed From Block Copolymers with Controlled Structure », *Langmuir*, vol. 25, n° 9, p. 5258‑5265, mai 2009.
[16] C. Chang *et al.*, « Temperature and pH Double Responsive Hybrid Cross-Linked Micelles Based on P(NIPAAm- *co* -MPMA)- *b* -P(DEA): RAFT Synthesis and "Schizophrenic" Micellization », *Macromolecules*, vol. 42, n° 13, p. 4838‑4844, juill. 2009.
[17] J. Du, H. Willcock, J. P. Patterson, I. Portman, et R. K. O'Reilly, « Self-Assembly of Hydrophilic Homopolymers: A Matter of RAFT End Groups », *Small*, vol. 7, n° 14, p. 2070‑2080, juill. 2011.

[18] F. Chen, D. Dai, J. Yang, Z. Fei, et M. Zhong, « Controlled Synthesis of Polyelectrolytes by 4-Cyanopentanoic Acid Dithiobenzoate Mediated RAFT Polymerization », *Journal of Macromolecular Science, Part A*, vol. 50, n° 9, p. 1002‑1006, janv. 2013.
[19] J. Chen, M. Liu, C. Gao, S. Lü, X. Zhang, et Z. Liu, « Self-assembly behavior of pH- and thermo-responsive hydrophilic ABCBA-type pentablock copolymers synthesized by consecutive RAFT polymerization », *RSC Advances*, vol. 3, n° 35, p. 15085, 2013.
[20] M. T. Savoji, S. Strandman, et X. X. Zhu, « Switchable Vesicles Formed by Diblock Random Copolymers with Tunable pH- and Thermo-Responsiveness », *Langmuir*, vol. 29, n° 23, p. 6823‑6832, juin 2013.
[21] Z. Ge et S. Liu, « Facile Fabrication of Multistimuli-Responsive Metallo-Supramolecular Core Cross-Linked Block Copolymer Micelles », *Macromolecular Rapid Communications*, vol. 34, n° 11, p. 922‑930, juin 2013.
[22] M. T. Savoji, S. Strandman, et X. X. Zhu, « Invertible vesicles and micelles formed by dually-responsive diblock random copolymers in aqueous solutions », *Soft Matter*, vol. 10, n° 32, p. 5886, juill. 2014.
[23] C. Ren, X. Jiang, G. Lu, X. Jiang, et X. Huang, « Construction of PIB-b-PDEAEMA well-defined amphiphilic diblock copolymers via sequential living carbocationic and RAFT polymerization », *Journal of Polymer Science Part A: Polymer Chemistry*, vol. 52, n° 10, p. 1478‑1486, mai 2014.
[24] D. B. Wright *et al.*, « Tuning the aggregation behavior of pH-responsive micelles by copolymerization », *Polym. Chem.*, vol. 6, n° 14, p. 2761‑2768, 2015.
[25] J. Zhou, W. Zhang, C. Hong, et C. Pan, « Silica Nanotubes Decorated by pH-Responsive Diblock Copolymers for Controlled Drug Release », *ACS Applied Materials & Interfaces*, p. 150206085211009, févr. 2015.
[26] M. Manguian, M. Save, et B. Charleux, « Batch Emulsion Polymerization of Styrene Stabilized by a Hydrophilic Macro-RAFT Agent », *Macromolecular Rapid Communications*, vol. 27, n° 6, p. 399‑404, mars 2006.
[27] S. R. Marek, C. A. Conn, et N. A. Peppas, « Cationic nanogels based on diethylaminoethyl methacrylate », *Polymer*, vol. 51, n° 6, p. 1237‑1243, mars 2010.
[28] A. Kawamura, Y. Hata, T. Miyata, et T. Uragami, « Synthesis of glucose-responsive bioconjugated gel particles using surfactant-free emulsion polymerization », *Colloids and Surfaces B: Biointerfaces*, vol. 99, p. 74‑81, nov. 2012.
[29] R. Tiwari, T. Heuser, E. Weyandt, B. Wang, et A. Walther, « Polyacid microgels with adaptive hydrophobic pockets and ampholytic character: synthesis, solution properties and insights into internal nanostructure by cryogenic-TEM », *Soft Matter*, vol. 11, n° 42, p. 8342‑8353, 2015.
[30] A. Pikabea, G. Aguirre, J. I. Miranda, J. Ramos, et J. Forcada, « Understanding of nanogels swelling behavior through a deep insight into their morphology », *Journal of Polymer Science Part A: Polymer Chemistry*, vol. 53, n° 17, p. 2017‑2025, sept. 2015.
[31] N. Sharifi-Sanjani, A. R. Mahdavian, et P. Bataille, « Emulsion polymerization of styrene and DEAEMA with a core-shell structure », *Journal of Applied Polymer Science*, vol. 78, n° 11, p. 1977‑1985, déc. 2000.
[32] A. Pikabea, J. Ramos, et J. Forcada, « Production of Cationic Nanogels with Potential Use in Controlled Drug Delivery », *Particle & Particle Systems Characterization*, vol. 31, n° 1, p. 101‑109, janv. 2014.
[33] F. M. J. Vallet, « Ethers of 7-hydroxy-coumarin useful as medicaments », US Patent 4,151,291, avr-1979.
[34] M. Wu *et al.*, « First multi-reactive dextran-based inisurf for atom transfer radical polymerization in miniemulsion », *Carbohydrate Polymers*, vol. 130, p. 141‑148, oct. 2015.

[35] S. R. Deshiikan et K. D. Papadopoulos, « Modified Booth equation for the calculation of zeta potential », *Colloid & Polymer Science*, vol. 276, n° 2, p. 117‑ 124, févr. 1998.
[36] C. Rouzes, R. Gref, M. Leonard, A. De Sousa Delgado, et E. Dellacherie, « Surface modification of poly(lactic acid) nanospheres using hydrophobically modified dextrans as stabilizers in an o/w emulsion/evaporation technique », *Journal of Biomedical Materials Research*, vol. 50, n° 4, p. 557‑ 565, juin 2000.
[37] K. Poltorak, A. Durand, M. Léonard, J.-L. Six, et C. Nouvel, « Interfacial click chemistry for improving both dextran shell density and stability of biocompatible nanocapsules », *Colloids and Surfaces A: Physicochemical and Engineering Aspects*, vol. 483, p. 8‑ 17, oct. 2015.
[38] L. M. Ramirez, J. Babin, A. Durand, J.-L. Six, et C. Nouvel, « Biocompatible dextran-covered nanoparticles produced by Activator Generated by Electron Transfer Atom Transfer Radical Polymerization in miniemulsion », *Colloids and Surfaces A: Physicochemical and Engineering Aspects*, vol. 486, p. 60‑ 68, déc. 2015.
[39] R. G. Strickley, « Solubilizing Excipients in Oral and Injectable Formulations », *Pharmaceutical Research*, vol. 21, n° 2, p. 201‑ 230, févr. 2004.
[40] A. Licea-Claveríe *et al.*, « The Use of the RAFT-Technique for the Preparation of Temperature/pH Sensitive Polymers in Different Architectures », *Macromolecular Symposia*, vol. 283‑ 284, n° 1, p. 56‑ 66, sept. 2009.
[41] L. Liu *et al.*, « Controlled polymerization of 2-(diethylamino)ethyl methacrylate and its block copolymer withN-isopropylacrylamide by RAFT polymerization », *Journal of Polymer Science Part A: Polymer Chemistry*, vol. 46, n° 10, p. 3294‑ 3305, mai 2008.
[42] K. E. Christodoulakis et M. Vamvakaki, « pH-Responsive Microgel Particles Comprising Solely Basic or Acidic Residues », *Macromolecular Symposia*, vol. 291‑ 292, n° 1, p. 106‑ 114, juin 2010.
[43] L. Barner, N. Zwaneveld, S. Perera, Y. Pham, et T. P. Davis, « Reversible addition-fragmentation chain-transfer graft polymerization of styrene: Solid phases for organic and peptide synthesis », *Journal of Polymer Science Part A: Polymer Chemistry*, vol. 40, n° 23, p. 4180‑ 4192, déc. 2002.
[44] M. Camail, H. Essaoudi, A. Margaillan, et J. L. Vernet, « Copolymérisation radicalaire de méthacrylates de 2-aminoéthyle avec le méthacrylate de méthyle », *European Polymer Journal*, vol. 31, n° 11, p. 1119‑ 1125, nov. 1995.
[45] A. Jhaveri, P. Deshpande, et V. Torchilin, « Stimuli-sensitive nanopreparations for combination cancer therapy », *Journal of Controlled Release*, vol. 190, p. 352‑ 370, sept. 2014.
[46] B. Chang, X. Sha, J. Guo, Y. Jiao, C. Wang, et W. Yang, « Thermo and pH dual responsive, polymer shell coated, magnetic mesoporous silica nanoparticles for controlled drug release », *Journal of Materials Chemistry*, vol. 21, n° 25, p. 9239, 2011.
[47] C. Y. Zhang, W. S. Wu, N. Yao, B. Zhao, et L. J. Zhang, « pH-sensitive amphiphilic copolymer brush Chol-g-P(HEMA-co-DEAEMA)-b-PPEGMA: synthesis and self-assembled micelles for controlled anti-cancer drug release », *RSC Adv.*, vol. 4, n° 76, p. 40232, août 2014.
[48] R. A. Siegel et B. A. Firestone, « pH-dependent equilibrium swelling properties of hydrophobic polyelectrolyte copolymer gels », *Macromolecules*, vol. 21, n° 11, p. 3254‑ 3259, nov. 1988.
[49] L. Du *et al.*, « The study of relationships between pKa value and siRNA delivery efficiency based on tri-block copolymers », *Biomaterials*, vol. 176, p. 84‑ 93, sept. 2018.
[50] E. Fuguet, C. Ràfols, M. Rosés, et E. Bosch, « Critical micelle concentration of surfactants in aqueous buffered and unbuffered systems », *Analytica Chimica Acta*, vol. 548, n° 1‑ 2, p. 95‑ 100, août 2005.

[51] J. Lazarovits, Y. Y. Chen, E. A. Sykes, et W. C. W. Chan, « Nanoparticle–blood interactions: the implications on solid tumour targeting », *Chem. Commun.*, vol. 51, n° 14, p. 2756‑2767, 2015.
[52] J. Tournebize, A. Boudier, A. Sapin-Minet, P. Maincent, P. Leroy, R. Schneider, « Role of Gold Nanoparticles Capping Density on Stability and Surface Reactivity to Design Drug Delivery Platforms » ACS Applied Materials & Interfaces, 4, (2012) 5790-5799. »
[53] J. Tournebize, A. Boudier, O. Joubert, H. Eidi, G. Bartosz, P. Maincent, P. Leroy, A. Sapin-Minet, « Impact of gold nanoparticle coating on redox homeostasis », International Journal of Pharmaceutics, 438, (2012) 107-116. »
[54] J. T. Ngo, B. M. Babin, J. A. Champion, E. M. Schuman, et D. A. Tirrell, « State-Selective Metabolic Labeling of Cellular Proteins », *ACS Chemical Biology*, vol. 7, n° 8, p. 1326‑1330, août 2012.
[55] J. M. Baskin *et al.*, « Copper-free click chemistry for dynamic in vivo imaging », *Proceedings of the National Academy of Sciences*, vol. 104, n° 43, p. 16793‑16797, oct. 2007.
[56] X. Ning, J. Guo, M. A. Wolfert, et G.-J. Boons, « Visualizing Metabolically Labeled Glycoconjugates of Living Cells by Copper-Free and Fast Huisgen Cycloadditions », *Angewandte Chemie International Edition*, vol. 47, n° 12, p. 2253‑2255, mars 2008.